

Research Article

Multi-Center Validation of Ladybug Beetle Optimized Convolutional Capsule Neural Networks with Explainable AI for Skin Cancer Classification Using Dermography Images

R Priyanka Pramila^{1*}, R Subhashini²

^{1*}Research Scholar, School of Computing, Sathyabama Institute of Science and Technology, Chennai, India.

E-Mail: priyankastephen1702@gmail.com

²Professor, Department of Computer Science Engineering, SRM Institute of Science and Technology, Ramapuram, Chennai, India. E-Mail: subhaagopi@gmail.com

Abstract

Skin cancer especially melanoma is one of the most common cancers around the world and needs early and accurate detection to improve the results for patients. Traditional methods for diagnosis have problems like being subjective and inconsistent which shows the need for better computer-based solutions. While deep learning techniques show promise in automating detection through dermoscopic image analysis existing models struggle with limited generalizability high computational demands and class imbalance in datasets. To address these limitations, this work proposes the Multi-Center Validation of Ladybug Beetle Optimized Convolutional Capsule Neural Networks with Explainable AI (LOCapsNet-XAI) for skin cancer classification using dermography images. The proposed workflow for skin cancer classification using LOCapsNet-XAI begins with the acquisition of multi-center clinical data contains diverse dermoscopic images from various healthcare institutions to create a representative training dataset. Next, image preprocessing techniques such as Anisotropic Diffusion and Kuwahara Filtering are employed to enhance image clarity by reducing noise while preserving important features like lesion boundaries. Following preprocessing, feature extraction is performed using the innovative Convolutional Capsule Neural Network (CapsNet) architecture, which effectively captures complex patterns and spatial relationships within the images. The model's parameters are then optimized using the Ladybug Beetle Optimization Algorithm (LBOA), which enhances the exploration and exploitation capabilities to improve classification performance. To foster trust in AI-assisted diagnoses, Explainable AI methodologies specifically Grad-CAM++ are integrated into the framework, that provides the clinicians with visual insights into the model's decision-making processes. Finally, the workflow culminates in the classification of skin lesions by accurately identifying them as benign or malignant and facilitating informed clinical decision making. The proposed LOCapsNet-XAI method achieves exceptional performance metrics including 99.992% accuracy; 99.99% precision; 99.988% specificity; 99.99% recall; 99.98% F1-score; 91ms computation time and an AUC value of 0.99. These findings underscore the capability of the proposed model to enhance early skin cancer detection and improve clinical outcomes. In conclusion, LOCapsNet-XAI represents a significant advancement in the automated detection of skin cancer facilitating reliable and interpretable diagnostics in diverse clinical environments.

Keywords: Multi-center clinical data, Anisotropic Diffusion and Kuwahara Filtering, Convolutional Capsule Neural Network, Ladybug Beetle Optimization Algorithm, Explainable AI, Grad-CAM++.

***Author for correspondence:** R Priyanka Pramila, E-Mail: priyankastephen1702@gmail.com

Received: 16/09/2024 Accepted: 22/10/2024

DOI: <https://doi.org/10.53555/AJBR.v27i3.3246>

© 2024 The Author(s).

This article has been published under the terms of Creative Commons Attribution-Noncommercial 4.0 International License (CC BY-NC 4.0), which permits noncommercial unrestricted use, distribution, and reproduction in any medium, provided that the following statement is provided. "This article has been published in the African Journal of Biomedical Research"

INTRODUCTION

Skin cancer is a malignant condition resulting from abnormal skin cell growth, and it is one of the most common cancers worldwide [1]. Each year, millions of people are affected due to prolonged exposure to ultraviolet (UV) radiation [2]. Among the various types of skin cancer, basal cell carcinoma (BCC), squamous cell carcinoma (SCC), and melanoma is the most common [3]. Melanoma is highly aggressive and responsible for most skin cancer-related deaths [4]. Early detection plays a crucial role in improving survival rates especially for melanoma, where timely diagnosis significantly enhances treatment outcomes [5-7]. Traditional diagnostic methods such as visual examination and biopsy are time-consuming, intrusive, and subject to varying interpretations, which leads to inconsistent outcomes [8-10]. While visual assessments by dermatologists remain the standard, these methods have limitations including human error and diagnostic inconsistency [11]. Distinguishing between malignant and benign lesions is challenging, which results in delayed diagnoses [12]. This issue is especially pronounced in regions with limited access to dermatological expertise [13-15]. Therefore, making early detection is difficult in certain populations.

To address these challenges, automated systems based on machine learning (ML) and deep learning (DL) have shown promise in improving skin cancer detection. These systems by analyzing dermoscopic images and classifying lesions as benign or malignant [16-18]. Despite their potential, current AI models face several limitations which includes restricted generalization capabilities, high computational demands, and difficulties integrating with existing clinical practices. A major issue with AI-based detection systems is their dependence on the data used for training. Models trained on non-diverse datasets struggle to generalize effectively to new cases, which limits their reliability across different populations [19]. Moreover, training and deploying deep learning models demand substantial computational cost, which is a barrier in settings with limited resources. The class imbalance in skin cancer datasets also result in models that are less effective at detecting early-stage malignant lesions [20-22].

One solution to these challenges is Explainable AI (XAI), which improves transparency by clarifying the decision-making process of AI models. This transparency fosters trust in the system and enables healthcare professionals to better understand and interpret AI predictions. XAI also helps to identify and rectify errors and biases in machine learning models, which reduces the probability of false positives and false negatives. By this, it improves the overall reliability of the model. XAI encourages collaboration between AI developers and clinicians by creating a shared framework for discussing results. This collaboration enhances system integration into clinical practice. Additionally, use of multi-center clinical data further enhances model generalization, reducing bias and promoting fairness across diverse populations.

Advancing AI models for skin cancer detection necessitates the integration of Explainable AI and multi-center clinical data. Explainable AI enhances model transparency, fostering trust among clinicians, while multi-center data improves generalization, reduces bias, and promotes fairness across

diverse populations. These combined approaches aim to create a reliable and effective AI-based tool for skin cancer detection, that can significantly improve patient outcomes. The contributions of the proposed LOCapsNet-XAI work are outlined below,

- The Convolutional Capsule Neural Networks optimized with the Ladybug Beetle Optimization algorithm (LOCapsNet) represents a novel approach designed to enhance feature extraction and classification capabilities in dermoscopic image analysis for skin cancer detection.
- The LOCapsNet model integrates Explainable AI (XAI) to improve transparency in the decision-making process, that enables healthcare professionals to better interpret and trust the system's predictions.
- The system is trained and validated on multi-center clinical data, which enhances generalization, reduces bias, and improves model performance across diverse populations.
- The proposed approach addresses the issue of class imbalance in skin cancer datasets, thereby improving the detection of early-stage malignant lesions.
- The system is optimized for computational requirements. So, it is feasible for deployment in settings with limited resources, thus increasing accessibility to early skin cancer diagnosis.

The subsequent sections of this manuscript detail the proposed LOCapsNet-XAI model for skin cancer diagnosis. Section 2 presents a systematic review of current skin cancer detection methods, emphasizing their advantages and limitations. Section 3 elaborates on the methodological framework of the LOCapsNet -XAI model, including its architecture and optimization strategies. Section 4 conducts an extensive evaluation of the model's performance, benchmarking it against existing state-of-the-art techniques. Finally, Section 5 discusses the results in depth, addressing the model's limitations and suggesting avenues for future research.

LITERATURE SURVEY

This section examines recent progress in deep learning approaches for the diagnosis of skin cancer using dermoscopic images. Below are several notable studies that illustrate diverse techniques and their contributions to enhancing diagnostic precision in this domain.

In 2022, Nigar, N., et.al [16] suggested explainable artificial intelligence (XAI) based system for skin lesion classification to enhance the accuracy of identifying various skin lesions. This approach assisted dermatologists in making informed diagnoses during the early stages of skin cancer. The XAI model was validated using the International Skin Imaging Collaboration (ISIC) 2019 dataset. The ResNet-18 model effectively classified eight types of skin lesions achieving classification accuracy, precision, recall, and F1 score of 94.47%, 93.57%, 94.01%, and 94.45% respectively. These predictions were further analyzed using the Explainable Artificial Intelligence (XAI) techniques such as local interpretable model-agnostic explanations (LIME) framework, which generated visual explanations that aligned with prior knowledge and established explanation

methodologies. The integration of explainability in the model enhanced its practical utility for clinical applications (ResNet-18-XAI). However, it has high error rate.

In 2024, Gautam, Y., et.al [17] presented FusionEXNet as an innovative and interpretable fused deep-learning model for skin cancer detection. FusionEXNet leveraged the strengths of EfficientNetV2S and XceptionNet architectures to extract robust features from dermoscopic images, that achieves superior performance compared to individual models. XceptionNet and EfficientNetV2S achieved accuracies of 88.82% and 88.01%, respectively, while FusionEXNet surpassed these results with an accuracy of 90.83%. To enhance model interpretability, Explainable Artificial Intelligence (XAI) techniques such as SmoothGrad and Faster Score-CAM were integrated for providing valuable insights into the decision-making process. The model was trained and evaluated using the extensive HAM10000 dataset, which consists of 10,015 high-resolution images across seven skin lesion categories. The EfficientNetV2S and XceptionNet-XAI model offered a reliable, accurate, and interpretable system for skin cancer detection. However, it has low accuracy.

In 2023, Mridha, K., et.al [18] suggested Enhanced Interpretability in Skin Cancer Classification via an Optimized Convolutional Neural Network for Intelligent Healthcare Solutions. It utilized the HAM10000 dataset and an optimized convolutional neural network (CNN) to identify seven forms of skin cancer. The model was trained using two optimization functions such as Adam and RMSprop along with three activation functions includes ReLU, Swish, and Tanh. Additionally, an explainable artificial intelligence (XAI) based skin lesion classification system was developed, incorporating Grad-CAM and Grad-CAM++ to elucidate the model's decisions. This CNN-Adam-RMSprop-XAI system assisted doctors in making informed diagnoses of skin cancer in its early stages. It achieves a classification accuracy of 82% and a loss accuracy of 0.47%. However, it has low F-Score value.

In 2023, Khater, T., et.al [19] developed machine learning-based model for skin cancer classification using preprocessed images from the PH² dataset. Initially, relevant features were extracted from these images, which provided more significant information than raw data. The XGBoost algorithm was employed for classification. It provides notable accuracy of 94% and an area under the curve (AUC) value of 0.9947. As a result, it effectively distinguishing the image between non-melanoma and melanoma skin cancers. Explainable artificial intelligence techniques, including partial dependence plots, permutation importance, and SHAP, were utilized to enhance interpretability. The analysis revealed that asymmetry and pigment network features emerged as the most critical factors influencing the classification of skin lesions. However, it has high computation time.

In 2024, Attallah, O., [20] developed Skin-CAD system to classify dermoscopic photographs of skin cancer (SC) into benign and malignant categories. It utilized four convolutional neural networks (CNNs) of varied topologies to extract features from the final pooling and fully connected layers, rather than relying solely on one layer. The system was validated using HAM10000 datasets. It employed Principal Component Analysis (PCA) for dimensionality reduction of pooling layer

features, thereby it minimizes the training complexity. Reduced pooling features were combined with fully connected features from each CNN integrating dual-layer features across the architectures. A feature selection step identified the most critical deep attributes for classification process. Predictions were analyzed using the Local Interpretable Model-agnostic Explanations (LIME) method to provide visual interpretations aligned with existing perspectives. However, it has low recall value.

In 2024, Hosny, K.M., et.al [21] proposed deep inherent learning method to classify seven types of skin lesions. Explainable AI (X-AI) was employed to elucidate decision-making processes at both local and global levels, that provides visual information and it enhanced the physician's trust. The challenging HAM10000 dataset served as the evaluation framework for this approach. A DIL-XAI framework was developed to aid medical practitioners in understanding the mechanisms of black-box AI models. However, it has low specificity value.

In 2023, Priyanka Pramila, R. and Subhashini, R., [22] proposed a fused deep convolutional neural network for the automated detection and classification of skin lesions using dermoscopic images (FDCNN-VGG19-ResNet152). The methodology involved preprocessing the images, followed by feature extraction utilizing the VGG19 and ResNet152 architectures. The obtained features were then input into a fused deep convolutional neural network for the classification task. Although the model demonstrated significant accuracy, its high computational demands constrained its effectiveness in real-time applications.

Problem Statement and Motivation

Automated systems employing machine learning (ML) and deep learning (DL) show promise in enhancing skin cancer detection through dermoscopic image analysis. Accurate and timely skin disease detection is crucial for effective treatment outcomes. However, existing AI models face challenges including limited generalization due to reliance on non-diverse training datasets, high computational demands, and difficulties in clinical integration. Class imbalance in skin cancer datasets further hampers the detection of early-stage malignant lesions [16-22]. To address these issues, Multi-Center Validation of Ladybug Beetle Optimized Convolutional Capsule Neural Networks with Explainable AI for Skin Cancer Classification Using Dermography Images is proposed. This study integrates Explainable AI (XAI) to enhance transparency and foster clinician trust while utilizing multi-center clinical data to improve generalization and fairness. The goal is to create a reliable AI tool that significantly improves patient outcomes in skin cancer diagnosis.

PROPOSED METHODOLOGY

In this section, the proposed methodology for skin cancer detection using a Ladybug Beetle Optimized Convolutional Capsule Neural Network (LOCapsNet) with Explainable AI is outlined. The workflow encompasses several key stages beginning with the acquisition of multi-center clinical data to ensure a diverse and representative dataset for model training and validation. This collaborative effort involves gathering

Multi-Center Validation of Ladybug Beetle Optimized Convolutional Capsule Neural Networks with Explainable Ai for Skin Cancer Classification Using Dermography Images

dermoscopic images from various institutions which facilitates a comprehensive dataset that spans a range of skin conditions, demographics, and skin types. The subsequent step involves preprocessing the collected images to ensure uniformity and eliminate noise which can obscure critical features such as lesion boundaries and textures. Techniques such as Anisotropic Diffusion and Kuwahara Filtering are employed to enhance image clarity while preserving vital diagnostic information. Following preprocessing the refined images serve as inputs for feature extraction and skin cancer detection through the innovative architecture of Convolutional Capsule Neural Networks (CapsNet). CapsNet's unique design allows it to effectively capture intricate patterns and spatial relationships within the dermoscopic images leading to improved classification accuracy. The model's parameters are then optimized using the Ladybug Beetles Optimization Algorithm (LBOA) which enhances exploration and exploitation capabilities in the parameter space while ultimately improving model performance. To further enhance the transparency and trustworthiness of the LOCapsNet model, Explainable AI techniques specifically Grad-CAM++ are integrated into the framework. This step provides clinicians with visual insights into the model's decision-making process while fostering confidence in AI-assisted diagnoses. Finally, the proposed methodology culminates in the classification of skin lesions ensuring precise detection and facilitating informed clinical decision-making. The block diagram illustrating the proposed

LOCapsNet-XAI framework is presented in Figure 1. A detailed description of each stage is given below,

Multi-Center Data Acquisition for Skin Cancer Detection

The collection of multi-center data is crucial for enhancing skin cancer detection through explainable AI methodologies. By collaborating with various institutions, a diverse dataset of dermoscopic images is assembled. It encompasses a wide range of skin conditions, demographics, and skin types. This diversity ensures that the developed models are generalized and applicable across different patient populations.

A key dataset in this domain is the International Skin Imaging Collaboration (ISIC) Dataset, which features over 482,781 dermoscopic images sourced from multiple international institutions. This expansive repository includes a broad spectrum of skin lesion types, enhancing the robustness and clinical applicability of models trained on it. The ISIC dataset is widely utilized in machine learning competitions focused on melanoma detection and is accessible via the ISIC Archive [23]. Another significant dataset is HAM10000, which comprises 10,015 images collected from various clinics in Austria and Australia. This dataset encompasses a variety of skin lesions, including melanoma, benign nevi, and seborrheic keratosis. Its extensive coverage of different lesion types and patient skin profiles serves as a valuable resource for developing models with high generalization capabilities. Therefore, it is widely adopted dataset in deep learning research for skin lesion classification available on Kaggle [24].

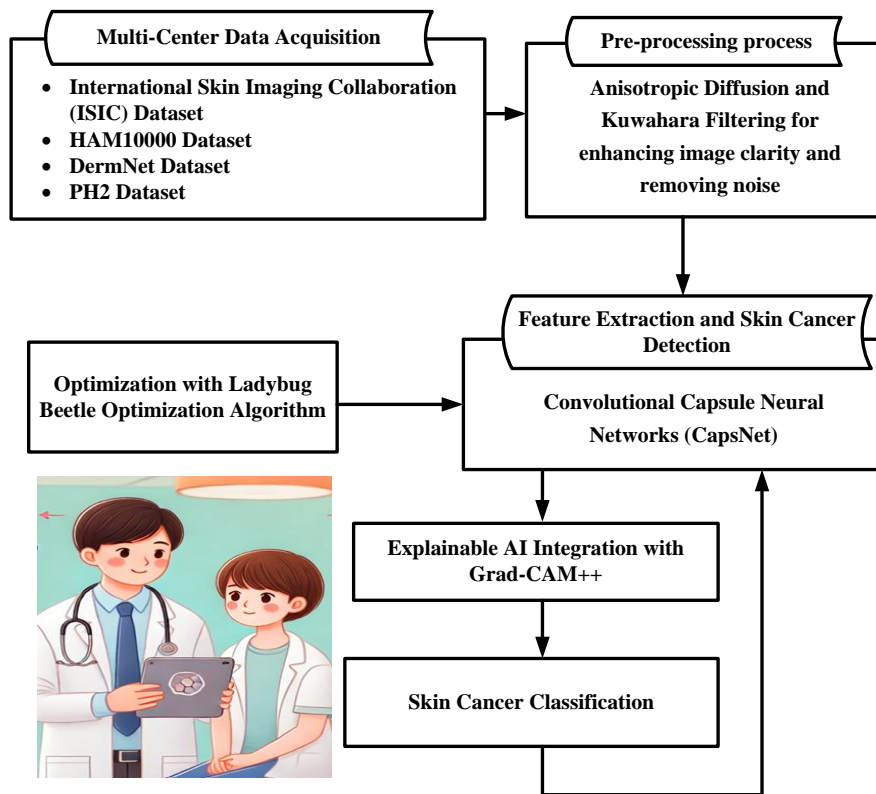


Figure 1: Block diagram of proposed LOCapsNet-XAI framework for skin cancer detection

The DermNet Dataset offers approximately 19,500 clinical and dermoscopic images from Australia, that covers a wide array of skin conditions, including melanoma. This dataset plays a significant role in training models for cancerous lesion detection and differentiating between benign and malignant skin conditions. It is publicly available on Kaggle [25].

Lastly, the PH₂ dataset is collected by the Dermatology Service of Hospital Pedro Hispano in Portugal, which comprises 200 dermoscopic images with each image representing one of three categories such as common nevi, atypical nevi, and melanoma [26]. This dataset provides a high-quality source of annotated images for skin cancer research. Its inclusion enhances the robustness of models trained for melanoma detection and provides a balanced set of cases for testing the performance of machine learning algorithms.

By integrating these datasets, a comprehensive and diverse collection of dermoscopic images is established for training and evaluating models aimed at skin cancer detection. This multi-center approach mitigates bias toward specific lesion types or demographics. Thereby, it improves the generalization and reliability of skin cancer detection systems.

Preprocessing process using Anisotropic Diffusion and Kuwahara Filtering

In multi-center data for skin cancer detection, preprocessing is essential to ensure uniformity and eliminate noise that ambiguous critical features like lesion boundaries and textures. Noise from various acquisition sources reduce the accuracy of machine learning models and introduce bias, thus making preprocessing a critical step to standardize images from diverse demographics and institutions. Techniques such as Anisotropic Diffusion and Kuwahara Filtering are particularly effective for this task [27], as it enhances image clarity while preserving vital diagnostic information like edges and textures.

Anisotropic Diffusion (AD) provides a nonlinear approach to filtering. By this, it balances the noise reduction with edge preservation. The traditional linear methods are blur uniformly across the image. But AD selectively smooths homogeneous regions while maintaining sharp boundaries. This is crucial for dermoscopic images where preserving lesion edges is necessary for accurate skin cancer detection. The diffusion process minimizes noise without distorting significant features, such as melanoma borders. Kuwahara Filtering further enhances the image by dividing it into local regions and applying an adaptive smoothing process. It calculates the mean and variance within sub-regions and selects the region with the smallest variance. By this, it ensures the structure of important features like lesions remains intact. This approach outperforms simple median or Gaussian filters, which often blur important diagnostic features in skin lesion images.

When combined these Anisotropic Diffusion and Kuwahara Filtering methods provide a robust preprocessing framework that removes noise, enhances structural details, and ensures the preservation of critical features across multi-center datasets.

Initially, Anisotropic diffusion operates by smoothing regions of the image based on gradient magnitude. By this, it preserves the edges where needed. The diffusion equation for AD is given in the subsequent equation (1)

$$\frac{\partial DI}{\partial t} = \text{div}[f|\nabla DI|^2] \times \nabla DI \quad (1)$$

Where DI represents the dermoscopic image, $f|\nabla DI|^2$ is the diffusivity function and it is mathematically given in the following equation (2)

$$f|\nabla DI|^2 = \frac{1}{1 + \frac{|\nabla DI|^2}{\alpha^2}} \quad (2)$$

Where α is the contrast parameter controlling diffusion across different regions of the image. For skin cancer detection, preserving the boundaries of lesions (high gradients) while smoothing noise within homogeneous areas (low gradients) is vital. This method ensures that key diagnostic features like lesion edges are intact while reducing irrelevant noise from diverse datasets. Then, Kuwahara filtering is applied to enhance local structural stability after AD. For each pixel, the image is divided into sub-regions, and the mean and variance are computed using equation (3-4)

$$\text{Mean}_{Reg} = \frac{1}{\text{Pixel}_{Reg}} \times \sum_{(a,b) \in \theta_{Reg}} \beta \times f(a,b) \quad (3)$$

$$\text{Variance}_{Reg}^2 = \frac{1}{\text{Pixel}_{Reg}} \times \sum_{(a,b) \in \theta_{Reg}} [\beta \times f(a,b) - \text{Mean}_{Reg}]^2 \quad (4)$$

Where $f(a,b)$ denotes the input dermoscopic image function; $\beta \times f(a,b)$ represents the pixel value in the dermoscopic image, Pixel_{Reg} is the number of pixels in region Reg . The region with the smallest variance is selected to update the pixel value, that ensures the noise reduction while retaining lesion boundaries and texture in the processed dermoscopic image.

The combined use of Anisotropic Diffusion and Kuwahara Filtering in multi-center skin cancer detection datasets enables effective noise reduction while preserving essential diagnostic features. This preprocessing approach enhances the model's ability to generalize across diverse datasets, improving the accuracy of skin cancer detection systems. Following preprocessing, the refined output serves as input for feature extraction and skin cancer detection utilizing Convolutional Capsule Neural Networks (CapsNet).

Feature extraction and skin cancer detection utilizing Convolutional Capsule Neural Networks (CapsNet)

The proposed Convolutional Capsule Neural Networks (CapsNet) offer significant advantages for feature extraction and skin cancer detection [28] compared to traditional neural networks. CapsNet has unique architecture, that employs capsules which effectively capture nuanced patterns and spatial relationships. By this, it enables the identification of delicate variations in skin lesions that are crucial for accurate diagnosis. CapsNet exhibits enhanced robustness to spatial transformations such as rotation and scaling. As a result, it ensures reliable classification results regardless of skin lesion position. This capability allows the networks to adapt to variations. Accordingly, it reduces the need for extensive data

augmentation. Additionally, CapsNet provides improved generalization, minimizes the risk of overfitting and allowing for better performance on unseen data. It also facilitates enhanced interpretability that helps clinicians understand the reasoning behind diagnoses, which is vital in medical applications. With lower computational complexity and the ability to learn features at multiple abstraction levels, CapsNet enables faster training and inference times. So, it is suitable for low-resource environments like mobile health applications. Furthermore, CapsNet handles occlusions and part deformations effectively. With this, it maintains the performance even in challenging scenarios. Overall, these benefits establish CapsNet as a powerful tool in skin cancer detection, which enhances the skin cancer diagnostic accuracy and supporting clinical decision-making.

The proposed CapsNet network is divided into two key components such as the feature extraction section and the skin cancer detection section. The primary function of the feature extraction section is to derive detailed features vital for the identification of skin cancer. This section employs a 2D Convolutional Neural Network (CNN) in conjunction with batch normalization (BN), ReLU activation, and four layers of Dense Convolutional (DC) blocks. Importantly, two DC blocks are followed by a Feature Attention block (FAB) and a Residual Block (RdB). The use of DC significantly decreases the number of parameters when compared to traditional CNN architectures, so it is well-suited for low-resource applications.

The FAB is instrumental in extracting robust features, while the RdB mitigates issues related to vanishing gradients. With this, it enhances both feature reuse and gradient flow. For the skin cancer detection section, global average pooling, dropout layers, dense layers, and softmax activation are employed to classify the features obtained. This structure minimizes both training and inference times. So, it is ideal for resource-constrained environments. The Architecture diagram of CapsNet network for Skin cancer classification is given in Figure 2.

To construct a compact deep learning model, Depthwise Separable Convolution (DC) is utilized as an efficient substitute for conventional CNN designs. This technique divides the convolution process into two phases namely depthwise convolution ($Dp_{convolution}$) and pointwise convolution ($Ps_{convolution}$). In depthwise convolution, each input channel receives a single convolutional kernel, while pointwise convolution employs a 1×1 convolution to merge the outputs from depthwise convolution. This approach significantly lowers the computational demand and reduces the overall model size. As a result, it is advantageous for applications on devices with limited resources. Mathematically, depthwise convolution is represented with the following equation (5)

$$Dp_{convolution}(K, F)_{a,b,u} = \sum_{kh,kw} K_{kh,kw} \times F_{a+kh,b+kw,u} \quad (5)$$

In this formulation, K indicates the convolution kernel and F denotes the feature map. The indices a, b and u represent the height, width, and depth of the feature map, respectively. kh, kw are the height and width of the kernel, respectively. Pointwise convolution is described by the following equation (6)

$$Ps_{convolution}(K, F)_{a,b} = \sum_u K_u \times F_{a,b,u} \quad (6)$$

Additionally, The Feature Attention Block (FAB) enhances the performance of CNNs by emphasizing the relationships among various local features. This block incorporates both average pooling and max pooling operations to extract spatial characteristics, which are subsequently combined into a unified feature set. The spatial attention feature map is defined by the following equation (7)

$$Sp(F) = \gamma \left[f_{3 \times 3} (F_{avg \ pooling} \oplus F_{Max \ pooling}) \right] \quad (7)$$

In this formulation, γ represents the sigmoid activation function, and $f_{3 \times 3}$ denotes a convolution operation with a kernel size of 3×3 . \oplus is the concatenation operator. The average pooling and max pooling are calculated based on the following equation (8-9)

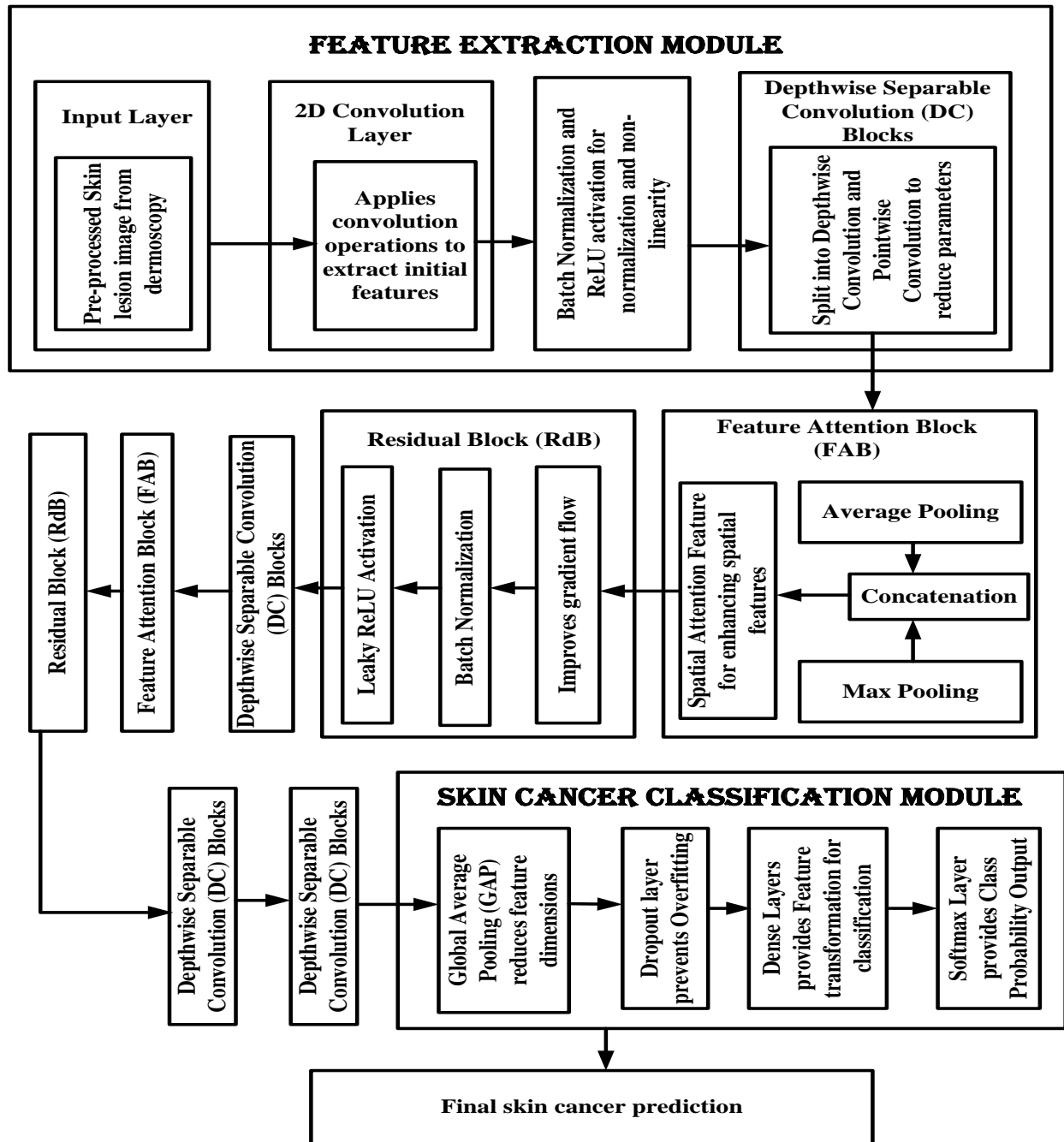


Figure 2: Architecture diagram of CapsNet network for Skin cancer classification

$$F_{avg\ pooling} = Avg\ pooling (F) \quad (8)$$

$$F_{Max\ pooling} = Max\ pooling (F) \quad (9)$$

The refined feature representation is derived through element-wise multiplication and it is mathematically expressed in the following equation (10)

$$\bar{F} = F \times Sp (F) \quad (10)$$

The Residual Block (RAB) addresses challenges associated with gradient propagation in deeper networks. This block consists of two convolutional layers, followed by batch normalization (BN) and a LeakyReLU activation layer. The residual connection is formulated using equation (11)

$$F^* = F \oplus f(F) \quad (11)$$

In this, F is the input feature and $f(F)$ represents the output from the convolutional layers. The LeakyReLU activation function is expressed using equation (12)

$$Leaky\ ReLU [F^*] = \{1; \text{if } F^* > 0 \delta; \text{Otherwise}\} \quad (12)$$

Here, δ signifies the leakage factor. After the feature extraction process, the model transitions into the classification phase, which leverages the features derived from the previous stages. This section utilizes global average pooling followed by dropout layers to enhance the robustness of the model against

overfitting. The pooled features are then fed into dense layers that ultimately produce class probabilities for skin cancer detection.

Here, Global average pooling serves to reduce the spatial dimensions of the feature maps, which generates a single feature vector per class. This process is defined mathematically with the equation (13)

$$GAP(F) = \frac{1}{Height \times Width} \sum_{a=0}^{Height} \sum_{b=0}^{Width} F_{a,b} \quad (13)$$

Where *Height* and *Width* represent the height and width of the feature maps, respectively. This operation minimizes the risk of overfitting and enhances the model's generalization capabilities. To further combat overfitting, a dropout layer is introduced. This layer randomly sets a fraction of the input units to zero during training. Thereby, it effectively prevents the model from relying too heavily on specific neurons. The dropout layer is expressed based on the following equation (14)

$$Out = F \odot Mask \quad (14)$$

In this context, *Mask* is a binary tensor generated randomly, and *Out* is the output after dropout. The output from the dropout layer is then passed through a series of dense layers. The final dense layer employs a softmax activation function to produce class probabilities for skin cancer detection across multiple categories. The softmax function is defined using equation (15)

$$\eta(B)_m = \frac{e^{B_m}}{\sum_z e^{B_z}} \quad (15)$$

for $m = 1, 2, \dots, Z$, where Z is the number of classes, and m is the input to the SoftMax layer. The classification output $Prob\left(\frac{Out}{F}\right)$ indicates the likelihood of each class given the input features F . The predicted class is determined using equation (16)

$$\hat{Out} = \arg \max_m \times Prob\left(\frac{Out_m}{F}\right) \quad (16)$$

This formulation facilitates the identification of skin cancer types, that ensures precise detection and classification. By this, the proposed CapsNet network effectively combines the feature extraction and classification through a series of advanced techniques, that offers a robust approach for skin cancer detection. The integration of Depth wise Separable Convolutions, Feature Attention, Residual Blocks, and sophisticated classification methods ensures high accuracy and efficiency, and it also suitable for practical applications in dermatological assessments.

Optimization algorithms play a vital role in enhancing the performance of Convolutional Capsule Neural Networks (CapsNet) for skin cancer detection. These algorithms accelerate training by minimizing the loss function and enabling quicker learning of optimal weights. Additionally, it reduces overfitting through regularization techniques which ensure effective generalization to unseen data. In resource-constrained environments optimization algorithms improve computational efficiency and maintain high accuracy without excessive resource demands.

Ladybug Beetle Optimization Algorithm for Optimizing the CapsNet Network

In this work, the Ladybug Beetle Optimization Algorithm (LBOA) is utilized to enhance the performance of Convolutional Capsule Neural Networks (CapsNet) for skin cancer detection. Inspired by the foraging behavior of ladybug beetles, it enhances exploration and exploitation capabilities within the model's parameter space. LBOA offers several advantages compared to other optimization algorithms as it efficiently navigates complex search spaces through its unique strategy. It exhibits strong convergence properties, so it provides quicker and more accurate solutions while effectively avoiding local optima. The adaptability of LBOA allows it to perform well across various optimization problems, and it requires fewer tuning parameters than traditional methods. This balanced approach improves the training process of CapsNet, leading to better accuracy and reliability in clinical applications. The Ladybug Beetle Optimization Algorithm (LBOA) is a bio-inspired metaheuristic algorithm modeled on the coordinated movement of ladybug beetles as they search for the warmest locations [29]. This optimization technique effectively balances exploration and exploitation in the search space to find optimal solutions. The pseudocode of Ladybug Beetle Optimization Algorithm (LBOA) for Optimizing CapsNet Network is given in Algorithm 1. Below is the step-by-step procedure for the LBOA to optimize the CapsNet network,

Step 1: Initialization

The initial population of $L(0)$ ladybug Beetles represent potential solutions (candidate hyperparameters and weights) for the CapsNet network. These ladybug Beetles are randomly distributed in the search space. Each ladybug Beetle's position corresponds to a unique configuration of CapsNet parameters. The objective function is evaluated for each ladybug Beetles representing the accuracy of CapsNet on the validation set. The population is sorted based on the objective function values.

Step 2: Fitness Function

The fitness function is designed to maximize CapsNet's performance, which is inversely related to the classification error. The fitness value *Fitness* (b_x) for each ladybug Beetles b_x is calculated using equation (17)

$$Fitness(b_x) = \frac{1}{1+ER(b_x)} \quad (17)$$

In this formulation, $ER(b_x)$ represents the classification error of the CapsNet network for the x^{th} ladybug Beetle's configuration. This fitness function ensures that configurations with lower errors have higher fitness values.

Step 3: Population Update

The position of each ladybug Beetles is updated based on neighboring solutions to explore better CapsNet configurations. The updated position for ladybug Beetles b_x in iteration $z + 1$ is computed using equation (18)

$$b_x(z+1) = b_x(z) + R \times [b_y(z) - b_x(z)] + R \times [b_y(z) - b_{y-1}(z)] + R \times |Cost_x|^{\frac{z}{L(z)}} \times b_x(z) \quad (18)$$

where $Cost_x$ is the ratio of the fitness value $Fitness(b_x)$ to the total fitness of all ladybug Beetles. R depicts the random number the values lie between 0 and 1. Roulette-wheel selection is applied to choose y , favoring solutions with better fitness values.

Step 4: Mutation Process

Here, mutation step is applied to maintain diversity and avoid premature convergence. The mutation affects a fraction of the hyperparameters or weights, with the number of mutated variables m_n is calculated by equation (19)

$$m_n = round(m \times \vartheta_n) \quad (19)$$

where m is the number of decision variables (parameters), and ϑ_n is the mutation rate. The mutated values are replaced with new random values within the feasible CapsNet parameter range.

Step 5: Population Size Update

The population of ladybug Beetles reduces gradually over iterations, that mimics the natural decline in ladybug Beetles numbers. The updated population size is calculated based on the following equation (20)

$$L(z + 1) = max \left\{ 0.25 \times L(0), round \left[L(z) - R \times L(z) \times \left[\frac{z}{z_{max}} \right] \right] \right\} \quad (20)$$

Where $L(0)$ is the initial population size, $L(z)$ is the population size at the current iteration z , z_{max} is the maximum number of iterations. This reduction prevents over-exploration in later stages of optimization.

Step 6: Termination

The LBO algorithm terminates once the maximum number of iterations or the maximum number of fitness evaluations is reached. The ladybug Beetles with the highest fitness value that is lowest CapsNet classification error is selected as the best solution, which provides the optimized hyperparameters and weights for the CapsNet network.

| Algorithm 1: Pseudocode of Ladybug Beetles Optimization Algorithm (LBOA) for Optimizing CapsNet Network |
|--|
| Initialize population $L(0)$ with random CapsNet configurations and evaluate the objective function. |
| Calculate fitness for each ladybug Beetles using equation (17). |
| Update each ladybug Beetles position by exploring neighboring solutions and improving configurations based on fitness values using equation (18) |
| Apply mutation to some parameters that introduces randomness to maintain diversity and prevent premature convergence using equation (19) |
| Gradually reduce the population size over iterations to focus the search using equation (20) and terminate when the best solution is found or iterations are complete. |

Integration of Explainable AI using Grad-CAM++ in LOCapsNet

Explainable Artificial Intelligence (XAI) is essential in medical applications particularly in skin cancer classification as it enhances the transparency and accountability of AI systems. By providing clear explanations for model predictions XAI fosters trust among healthcare professionals and aids in clinical decision-making. One effective technique for achieving explainability in LOCapsNet networks is Grad-CAM++ [18]. Grad-CAM++ addresses limitations of the original Grad-CAM method by delivering refined visual explanations of the model's predictions. While Grad-CAM highlights significant regions in the input image it produces coarse heatmaps that do not capture fine details. Grad-CAM++ addresses this limitation by incorporating guided backpropagation to create more detailed feature maps allowing for the preservation of spatial information. This advancement is particularly valuable in multi-class scenarios where distinct visualizations for different classes enhance interpretability.

Grad-CAM++ offers several advantages in skin cancer classification that significantly enhance its utility in medical applications. By generating detailed heatmaps, Grad-CAM++ provides clinicians with precise visualizations of the critical areas influencing the model's predictions, thereby it improves the diagnostic accuracy. It has the capability to effectively

handle multiple classes and allows for the differentiation of various skin cancer types that facilitates more accurate diagnoses. Additionally, Grad-CAM++ enhances the model's transparency, which promotes clinician confidence in AI-assisted diagnoses. The insights gained from Grad-CAM++ visualizations also serve as valuable tools for guiding the debugging and refinement of the model, that leads to improved performance overall.

The implementation of Grad-CAM++ within the Ladybug Beetles Optimized Convolutional Capsule Neural Networks (LOCapsNet) framework is executed into three key steps. The detailed explanation is given below,

Step 1: Gradient Calculation

In this step, the gradient of the output score G_s with respect to the feature map activations A_p from the last convolutional layer is calculated. For instance, if G_s corresponds to the score for a specific class the gradients are expressed mathematically by the equation (21)

$$\frac{\partial G_s}{\partial A_p} = \frac{\partial G_s}{\partial A_1} + \frac{\partial G_s}{\partial A_2} + \frac{\partial G_s}{\partial A_3} \quad (21)$$

Step 2: Deriving Alpha Values

This step involves obtaining the neuron importance weights \mathfrak{N}_p^s by averaging the gradients over the spatial dimensions of the feature maps. It is represented in the equation (22)

$$\mathfrak{N}_p^s = \frac{1}{E} \times \sum_u \sum_v \frac{\partial G_s}{\partial A^{uv}} \quad (22)$$

Here, E denotes the total number of pixels in the feature map. u and v represent the spatial dimensions (width and height) of the feature map. The averaged gradient values for each feature map are calculated in the following equation (23-25)

$$\frac{\partial G_s}{\partial A_1} = \text{averaging}[\mathfrak{N}_{p=1}^s] \quad (23)$$

$$\frac{\partial G_s}{\partial A_2} = \text{averaging}[\mathfrak{N}_{p=2}^s] \quad (24)$$

$$\frac{\partial G_s}{\partial A_3} = \text{averaging}[\mathfrak{N}_{p=3}^s] \quad (25)$$

Step 3: Generating the Final Heatmap

In this step, final Grad-CAM++ heatmap is generated using a weighted combination of the feature map activations, where the weights are derived from the calculated alpha values. It is mathematically represented in the following equation (26)

$$L_S^{Grad-CAM++} = ReLU \sum_p \mathfrak{N}_p^s \times A_p \quad (26)$$

This equation (26) expresses the final heatmap as a combination of weighted feature maps, highlighting the region's most influential in the skin cancer classification decision. Integrating Grad-CAM++ into the LOCapsNet framework significantly enhances interpretability in skin cancer classification. By providing clear insights into model predictions, Grad-CAM++

builds confidence among clinicians and supports informed decision-making. Furthermore, the deployment of Grad-CAM++ aids in understanding model behavior and facilitates continuous improvement, which is crucial in medical applications where precision is paramount.

RESULTS AND DISCUSSION

This section outlines the performance evaluation of the LOCapsNet-XAI framework, designed for skin cancer classification using dermography images. The LOCapsNet-XAI framework was implemented in Python, and experiments were conducted using NVIDIA GeForce GTX 1650 GPUs on a personal computer equipped with an Intel Core i5 processor operating at 3.2 GHz and 16 GB of RAM. Rigorous testing was performed to evaluate the framework's effectiveness in identifying and classifying different types of skin cancer. The dataset was divided into training (70%), validation (15%), and testing (15%) sets, facilitating a comprehensive assessment of model performance. Various performance metrics including accuracy, precision, recall, F1 score, specificity, ROC, and computation time were calculated to provide an extensive evaluation of the model's capabilities. Experimental results indicated that the LOCapsNet-XAI framework outperformed conventional methods including ResNet-18-XAI, EfficientNetV2S, XceptionNet-XAI, and CNN-Adam-RMSprop-XAI. The hyperparameter settings for the proposed LOCapsNet-XAI framework are detailed in Table 1. The Visualization of output results from the LOCapsNet-XAI method is given in Figure 3.

Table 1: Hyperparameter Settings for the Proposed LOCapsNet-XAI Framework

| Hyperparameter | Value |
|--|--|
| Learning Rate | 0.001 |
| Batch Size | 64 |
| Epochs | 1000 |
| Optimizer | Ladybug Beetle Optimization Algorithm (LBOA) |
| Dropout Rate | 0.2 |
| Activation Function | ReLU |
| Initial Learning Rate | 0.001 |
| Decay Rate | 0.9 |
| Minimum Learning Rate | $1e^{-5}$ |
| Momentum | 0.9 |
| Kernel Size (Convolutional Layers) | 3×3 |
| Number of Filters (Convolutional Layers) | 32, 64, 128, 256 |
| Capsule Dimensions | 8 |
| Routing Iterations | 3 |
| Primary Capsule Length | 16 |
| Input dermography Image Size | 224×224 |
| Feature Attention Block | Sigmoid |
| Residual Block | Leaky ReLU |
| LBOA Population Size | 50 |
| LBOA Maximum Iterations | 100 |
| LBOA Mutation Rate | 0.1 |

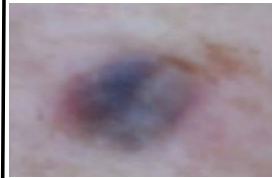
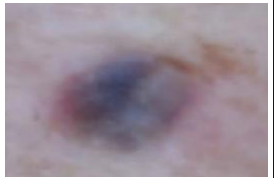
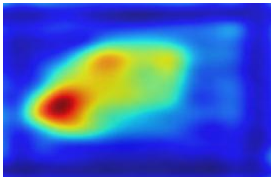


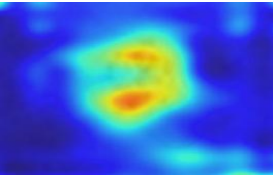


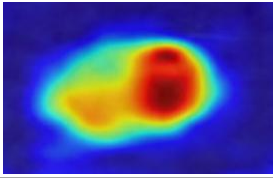
| Input Image | Pre-processing Output | Grad-CAM++ Output | Classification Output |
|---|---|--|-----------------------------|
|  |  |  | Malignant |
|  |  |  | Vascular Lesion |
|  |  |  | Basal Cell Carcinoma |

Figure 3: Visualization of output results from the LOCapsNet-XAI method

Performance Metrics

This section delineates the performance metrics employed to evaluate the Convolutional Capsule Neural Network optimized with the Ladybug Beetle Optimization algorithm, integrated with explainable AI for multi-center clinical application in skin cancer detection.

Accuracy

Accuracy measures the proportion of correctly classified instances among the total instances in the dataset. The relevant expressions are articulated in Equation (27).

$$Accuracy = \frac{TP+TN}{TP+FP+TN+FN} \quad (27)$$

Where True Positive (TP) refers to cases where skin cancer is correctly identified by the model as malignant lesions; True Negative (TN) represents instances where non-cancerous lesions are correctly classified as benign by the model; False Positive (FP) indicates cases where benign lesions are mistakenly classified as malignant by the model; False Negative (FN) refers to instances where actual malignant lesions are incorrectly identified as benign by the model.

Precision

Precision evaluates the accuracy of the positive predictions made by the model. It indicates the proportion of true positive results in all positive predictions. The relevant expressions are articulated in Equation (28)

$$Precision = \frac{TP}{(TP+FP)} \quad (28)$$

Recall

Sensitivity is also known as recall, that quantifies the ability of the model to correctly identify positive instances. It reflects the proportion of actual positives that are correctly identified. The relevant expressions are articulated in Equation (29)

$$Recall = \frac{TP}{(TP+FN)} \quad (29)$$

F1 Score

The F-score is the harmonic mean of precision and recall. The relevant expressions are articulated in Equation (30)

$$F1\ Score = \frac{2 \times (Precision \times Recall)}{(Precision + Recall)} \quad (30)$$

Specificity

Specificity measures the proportion of actual negatives that are correctly identified. It indicates how well the model avoids false positives. The relevant expressions are articulated in Equation (31)

$$Specificity = \frac{TN}{(TN+FP)} \quad (31)$$

Computation time

Computation time refers to the total time taken by the model to process the input data, perform inference, and output the results. It is typically measured in seconds or milliseconds.

4.2 Performance Analysis

The figure 4-10 offers a comparative analysis of the proposed LOCapsNet-XAI framework outperformed traditional methods, such as ResNet-18-XAI [16], EfficientNetV2S and XceptionNet-XAI [17] and CNN-Adam-RMSprop-XAI [18] respectively.

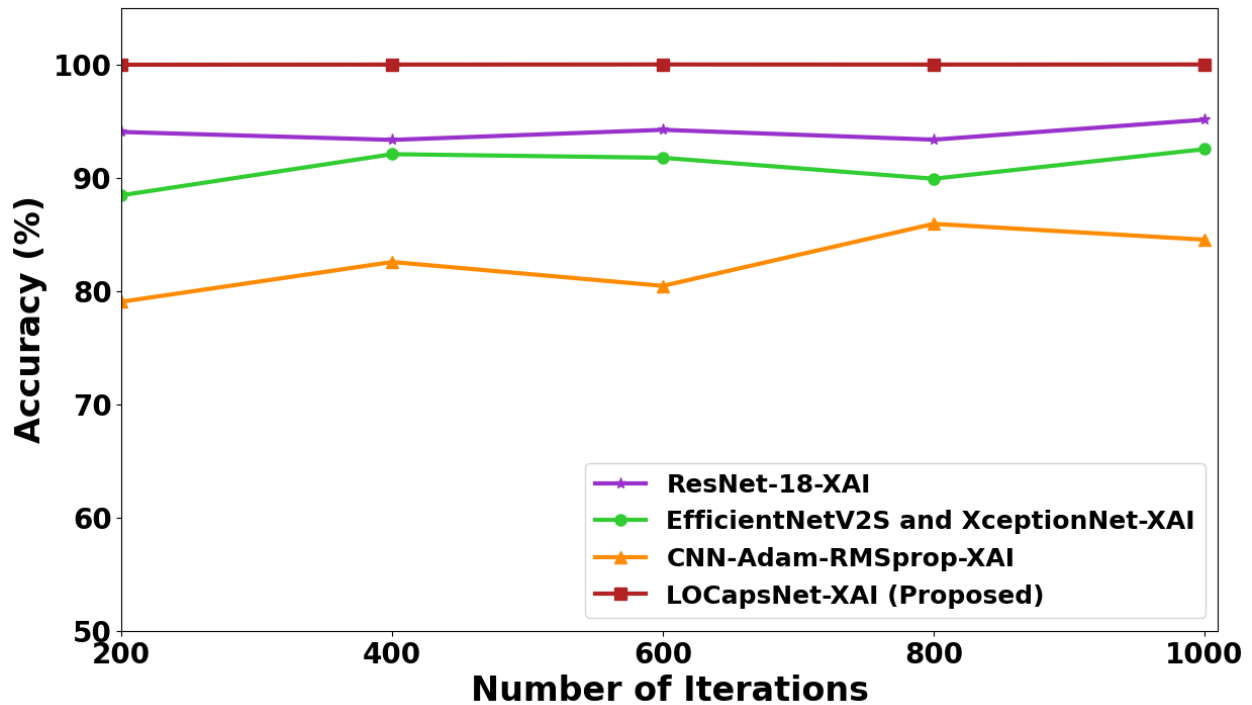


Figure 4: Accuracy Analysis for Skin Cancer Classification

Figure 4 depicts the accuracy analysis for skin cancer classification using the proposed LOCapsNet-XAI method illustrating its superior performance compared to established models. The proposed LOCapsNet-XAI method attains 6.31%, 13.03% and 26.47% high accuracy at iteration 200; 7.12%, 8.59% and 21.11% high accuracy at iteration 400; 6.12%, 8.97% and 24.3% high accuracy at iteration 600; 7.101%, 11.21% and 16.36% high accuracy at iteration 800; 5.13%, 8.08% and 18.301% high accuracy at iteration 1000 when compared to existing methods such as ResNet-18-XAI, EfficientNetV2S, XceptionNet-XAI, and CNN-Adam-

RMSprop-XAI. These results indicate that the LOCapsNet-XAI model not only enhances accuracy but also exhibits significant stability across varying iteration counts. As a result, it demonstrates its capability in the realm of skin cancer detection. By leveraging CapsNet, the method effectively captures spatial relationships within dermoscopic images, that are crucial for discerning subtle differences between malignant and benign lesions. Furthermore, the integration of explainable AI within LOCapsNet-XAI provides transparency in the decision-making process, which enhances the clinician's confidence and understanding of the model's outputs.

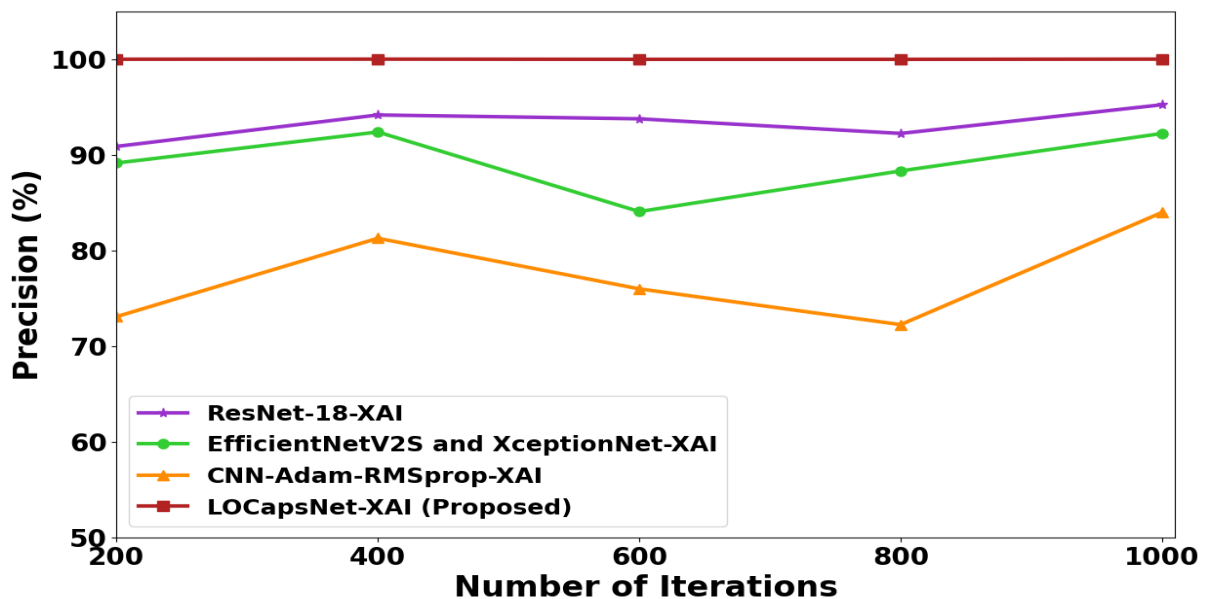


Figure 5: Precision Analysis for Skin Cancer Classification

Figure 5 illustrates the precision analysis for skin cancer classification using the proposed LOCapsNet-XAI method. At iteration 200, the model achieves precision levels of 10.03%, 12.17%, and 36.84%. Precision improves at iteration 400, yielding results of 6.202%, 8.24%, and 23.04%. Further enhancement is observed at iteration 600, where precision reaches 6.63%, 18.93%, and 31.58%. At iteration 800, precision metrics are recorded at 8.402%, 13.21%, and 38.39%. Finally, at iteration 1000, precision values are noted at 5.008%, 8.42%, and 19.09%. The precision values recorded for the LOCapsNet-XAI method highlight its superiority over established techniques such as ResNet-18-XAI, EfficientNetV2S, XceptionNet-XAI, and CNN-Adam-RMSprop-XAI. The observed precision values reflect the model's capability to minimize false positive rates, which is crucial for maintaining the reliability of skin cancer detection systems. High precision is particularly important in clinical settings where false positives lead to unnecessary anxiety and additional invasive procedures for patients. The proposed CapsNet architecture's ability to capture spatial hierarchies and relationships within dermoscopic images allows for a nuanced understanding of lesion

characteristics. This spatial awareness is vital in differentiating subtle distinctions between malignant and benign lesions. Furthermore, the incorporation of explainable AI in the LOCapsNet-XAI framework provides transparency regarding the process of predictions, that enables the clinicians to understand the basis for the model's decisions. This understanding is crucial for enhancing clinician trust in automated systems and promoting collaborative decision-making in patient care. The multi-center validation of the LOCapsNet-XAI method confirms its robustness and applicability across varied patient demographics. This adaptability is essential for real-world implementation in dermatology, where variations in skin types and lesion presentations are common. Overall, the findings from the precision analysis of LOCapsNet-XAI emphasize its potential to improve clinical practices in skin cancer classification significantly. By providing a reliable and transparent tool, this model enhances diagnostic accuracy and contribute to better patient outcomes. It highlights the critical need for precise diagnostic tools in the healthcare system.

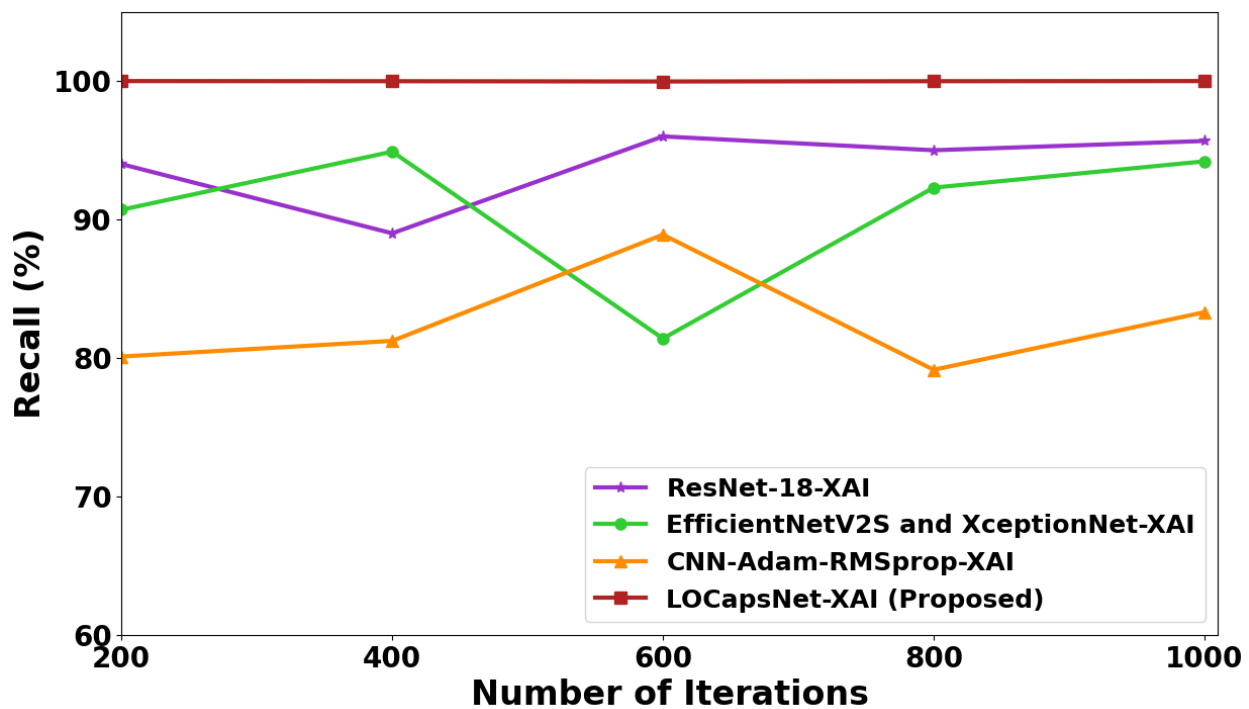


Figure 6: Recall Analysis for Skin Cancer Classification

Figure 6 illustrates the Recall Analysis for the skin cancer classification task of the proposed LOCapsNet-XAI method compared to existing models including ResNet-18-XAI, EfficientNetV2S, XceptionNet-XAI, and CNN-Adam-RMSprop-XAI. The results demonstrate that the LOCapsNet-XAI method consistently achieves superior Recall rates across various iterations, that showcases its effectiveness in detecting skin cancer lesions. At iteration 200, the LOCapsNet-XAI method achieves Recall values of 6.38%, 10.25%, and 24.84%, that indicates its capability to identify different categories of skin cancer effectively. As the training progresses to iteration

400, the Recall performance remains competitive with values of 12.34%, 5.36%, and 23.09%. This suggests that the model is not only maintaining but also improving its sensitivity to various skin cancer types over successive iterations. At iteration 600, the Recall performance remains competitive with values of 4.13%, 22.81%, and 12.45%. Moving to iteration 800, the LOCapsNet-XAI method exhibits a noteworthy improvement with Recall rates of 5.25%, 8.33%, and 26.34%. This enhancement indicates effective learning from the training data, as the model fine-tunes its parameters and improves its predictive capabilities. Finally, at iteration 1000, the model

achieves Recall values of 4.52%, 6.15%, and 20.04%. Overall, it shows that the proposed LOCapsNet-XAI method maintains a high level of Recall throughout the training process compared with the existing methods like ResNet-18-XAI,

EfficientNetV2S, XceptionNet-XAI, and CNN-Adam-RMSprop-XAI. This comparison underscores the effectiveness of the LOCapsNet-XAI method as a reliable tool for skin cancer classification.

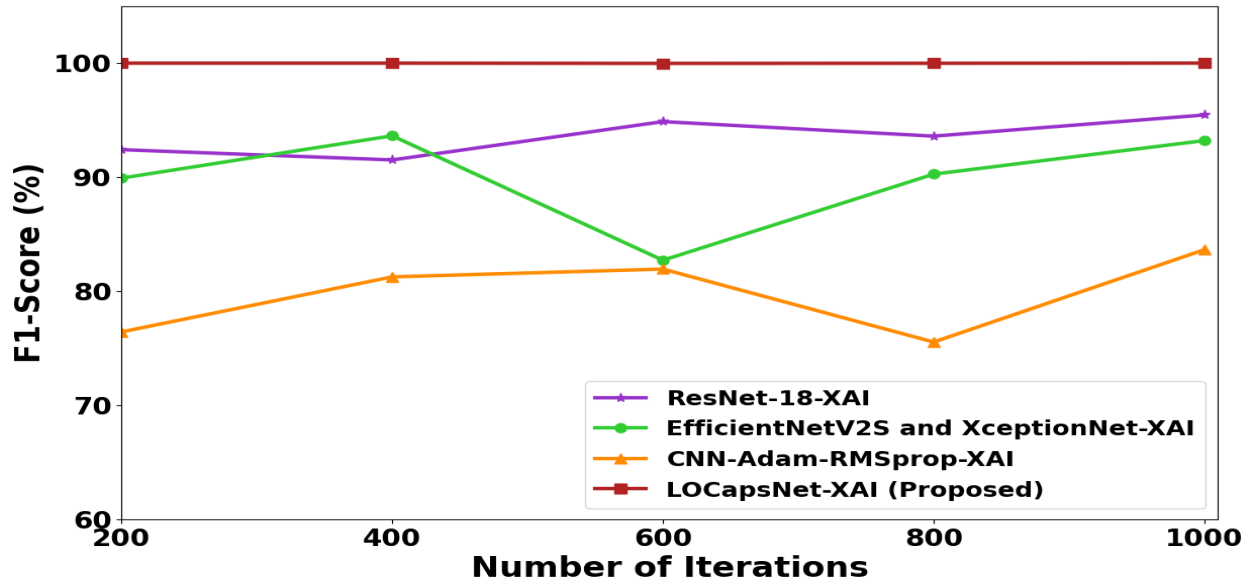


Figure 7: F1-Score Analysis for Skin Cancer Classification

Figure 7 depicts the F1-Score Analysis for Skin Cancer Classification. The proposed LOCapsNet-XAI method attains 8.209%, 11.21% and 30.84% high F1-Score at iteration 200; 9.27%, 6.805% and 23.07% high F1-Score at iteration 400; 5.38%, 20.87% and 22.01% high F1-Score at iteration 600; 6.82%, 10.77% and 32.37% high F1-Score at iteration 800; 4.76%, 7.29% and 19.56% high F1-Score at iteration 1000 compared with existing methods like ResNet-18-XAI, EfficientNetV2S and XceptionNet-XAI and CNN-Adam-RMSprop-XAI respectively. The results highlight the superior

performance of the LOCapsNet-XAI method in skin cancer classification, that showcases its effectiveness in recognizing and distinguishing various skin cancer types using dermography images. This performance positions LOCapsNet-XAI as a reliable tool for enhancing diagnostic accuracy with significant implications for clinical practice and patient care. The incorporation of explainable AI further ensures that clinicians interpret the model's predictions, that fosters trust in its applicability for real-time decision-making in dermatological assessments.

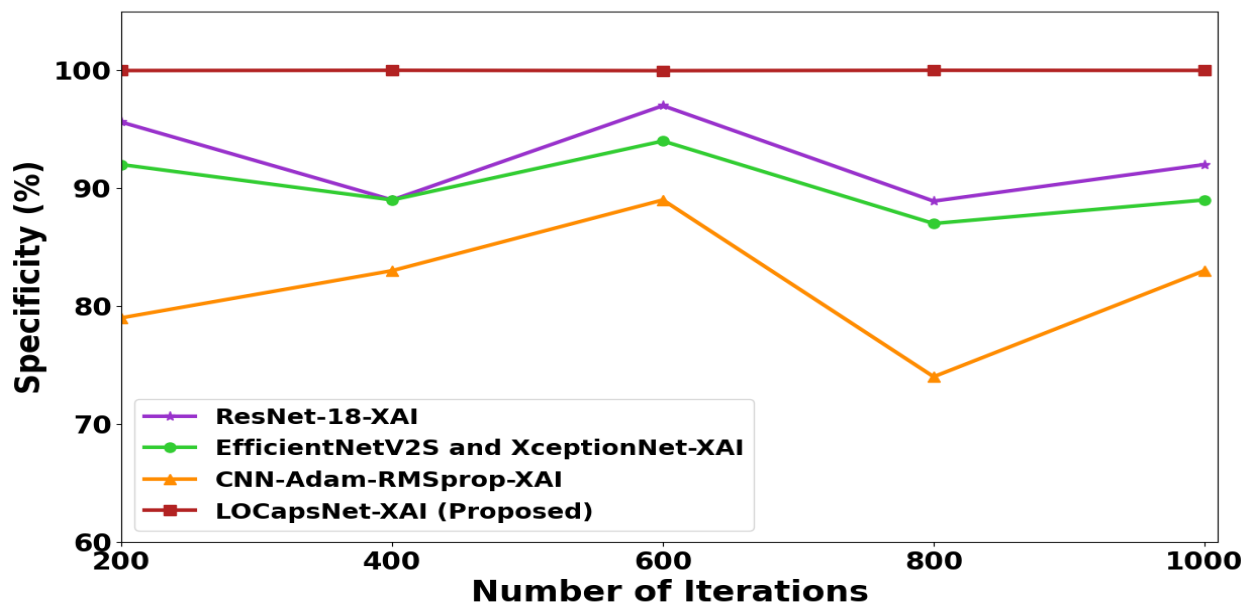


Figure 8: Specificity Analysis for Skin Cancer Classification

Figure 8 depicts the Specificity Analysis for Skin Cancer Classification. The proposed LOCapsNet-XAI method attains 4.58%, 8.67% and 26.55% high Specificity at iteration 200; 12.35%, 12.35% and 20.48% high Specificity at iteration 400; 3.06%, 6.35% and 12.32% high Specificity at iteration 600; 12.48%, 14.94% and 35.13% high Specificity at iteration 800; 8.68%, 12.34% and 20.46% high Specificity at iteration 1000

compared with existing methods like ResNet-18-XAI, EfficientNetV2S and XceptionNet-XAI and CNN-Adam-RMSprop-XAI respectively. These results indicate a strong potential for the model to reduce false positives while maintaining accurate cancer detections. By this, it emphasizes the precision and reliability of the LOCapsNet-XAI method in detecting skin cancer.

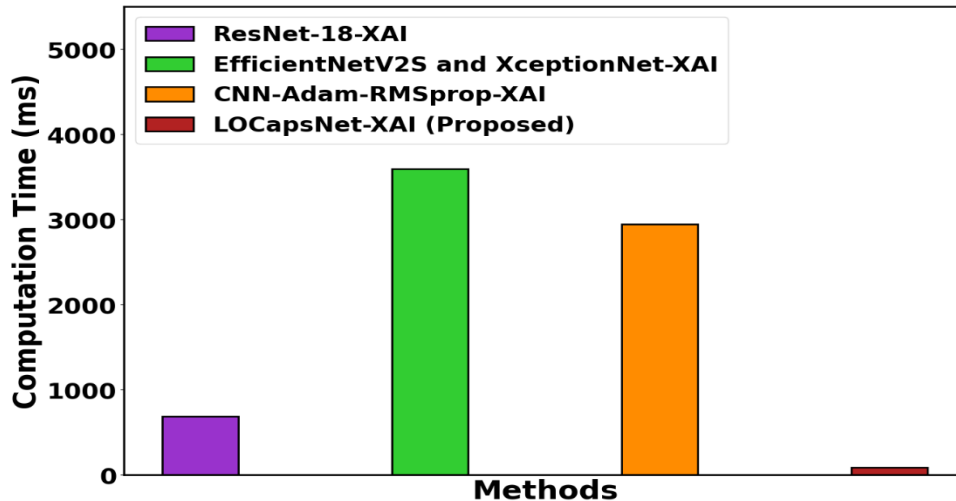


Figure 9: Computation time Analysis for Skin Cancer Classification

Figure 9 depicts the Computation time Analysis for Skin Cancer Classification. The proposed LOCapsNet-XAI method attains 86.79%, 97.46% and 96.907% low Computation time compared with existing methods like ResNet-18-XAI, EfficientNetV2S and XceptionNet-XAI and CNN-Adam-RMSprop-XAI respectively. This reduction in computation time is attributed to several factors inherent to the LOCapsNet-XAI architecture. Firstly, the model's lightweight design incorporates a novel CapsNet framework, which facilitates more efficient feature extraction and reduces the complexity associated with traditional convolutional neural networks. Furthermore, the integration of explainable artificial intelligence (XAI) mechanisms within LOCapsNet-XAI enhances interpretability

while maintaining low computational overhead. This is crucial in medical applications, where understanding model decisions is essential for gaining trust from clinicians and ensuring patient safety. The implications of these findings are significant for clinical settings. The reduced computation time not only accelerates the diagnostic process but also allows for the implementation of real-time skin cancer detection systems. This efficiency led to timely interventions and improved patient outcomes particularly in high-throughput environments where rapid decision-making is paramount. Overall, the computation time analysis highlights the advantages of the LOCapsNet-XAI method in the domain of skin cancer classification.

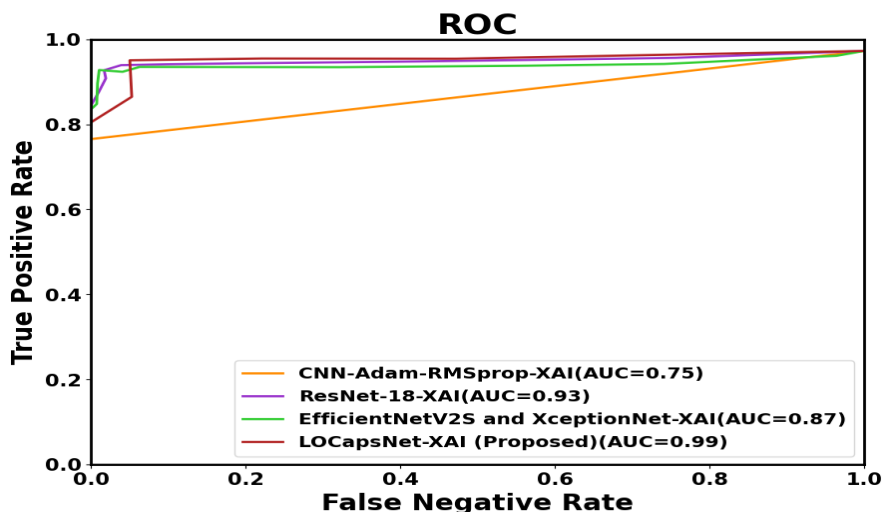


Figure 10: RoC analysis for Skin Cancer Classification

Figure 10 illustrates the Receiver Operating Characteristic (RoC) analysis for Skin Cancer Classification. The proposed LOCapsNet-XAI framework demonstrates notable improvements in the Area Under the Curve (AUC) values, achieving increases of 6.45%, 13.79% and 32% compared to the existing methods, including ResNet-18-XAI, EfficientNetV2S and XceptionNet-XAI and CNN-Adam-RMSprop-XAI respectively. The RoC curve illustrates the trade-off between sensitivity (true positive rate) and specificity (false positive rate) across various threshold settings. A higher AUC value indicates better model performance in distinguishing between positive and negative cases of skin cancer. The notable increases in AUC values for LOCapsNet-XAI highlight its superior capability in accurately identifying skin lesions, which is critical in clinical diagnostics. These advancements in AUC values not only signify the efficacy of the LOCapsNet-XAI framework in detecting skin cancer but also underscore its potential to improve diagnostic accuracy in real-world applications. This enhanced performance in AUC metrics is essential for building clinician confidence in automated systems, that facilitates quicker and more reliable decision-making in patient care. Overall, the RoC analysis for LOCapsNet-XAI illustrates its competitive edge over established methods, that paves the way for advancements in skin cancer detection and contributing to more effective and efficient healthcare solutions.

Discussion

The results presented in Figures 4 to 10 highlight the robust performance of the proposed LOCapsNet-XAI framework for skin cancer classification, that demonstrates significant advancements over traditional models such as ResNet-18-XAI, EfficientNetV2S and XceptionNet-XAI and CNN-Adam-RMSprop-XAI. The accuracy analysis indicates that the LOCapsNet-XAI consistently achieves higher accuracy levels across various iterations. This superior performance is attributed to the architecture's unique ability to capture spatial relationships in dermoscopic images through LOCapsNet, that enhances the model's capability to differentiate between malignant and benign lesions. Precision is a critical metric in medical diagnostics, as it reflects the proportion of true positive results in the context of predicted positives. The precision analysis demonstrates that LOCapsNet-

XAI maintains high precision across iterations, that significantly reduces the risk of false positives. This finding is particularly important in clinical settings, where unnecessary anxiety and invasive procedures due to misdiagnosis adversely affect patient outcomes. The model's ability to sustain high precision values across iterations indicates its reliability and potential for real-world application in dermatology. Recall or sensitivity is another vital metric in the context of skin cancer detection, where the aim is to identify as many positive cases as possible. The recall rates achieved by LOCapsNet-XAI are indicative of its effectiveness in detecting various types of skin cancer lesions, that highlights its potential to minimize missed diagnoses. High recall values suggest that the model captures a broad spectrum of skin cancer types, which is essential for improving early detection and treatment outcomes.

The F1-score, which balances precision and recall further substantiates the strength of the LOCapsNet-XAI framework. The consistently high F1-scores across iterations reinforce the model's reliability and effectiveness in providing accurate classifications. This balance between precision and recall is crucial for ensuring that the diagnostic process is both sensitive and specific, ultimately enhancing clinical decision-making. Specificity analysis indicates that LOCapsNet-XAI also excels in accurately identifying negative cases, thus reducing the likelihood of false negatives. This aspect of performance is particularly important in avoiding unnecessary follow-up procedures for patients who do not have skin cancer. The model's ability to achieve high specificity rates emphasizes its potential for practical application in dermatological assessments, that enables the clinicians to make informed decisions with greater confidence.

The integration of explainable AI (XAI) within the LOCapsNet-XAI framework adds an additional layer of value, which provides insights into the decision-making processes of the model. By elucidating the model's prediction processes, XAI enhances clinician trust and facilitates a collaborative approach to patient care. This transparency is critical in medical applications, as understanding the rationale behind a diagnosis significantly influence treatment pathways. Overall, the LOCapsNet-XAI framework represents a promising advancement in the field of skin cancer classification.

Table 2: Overall performance metrics for skin cancer detection

| | ResNet-18-XAI | EfficientNetV2S and XceptionNet-XAI | CNN-Adam-RMSprop-XAI | LOCapsNet-XAI (Proposed) |
|-----------------------|----------------------|--|-----------------------------|---------------------------------|
| Accuracy (%) | 94.01 | 90.94 | 82.5 | 99.99 |
| Precision (%) | 93.25 | 89.22 | 77.3 | 99.99 |
| Specificity (%) | 92.5 | 90.2 | 81.6 | 99.98 |
| Recall (%) | 93.93 | 90.7 | 82.53 | 99.99 |
| F1 Score | 93.56 | 89.94 | 79.75 | 99.99 |
| Computation time (ms) | 689 | 3594 | 2943 | 91 |
| RoC | 0.93 | 0.87 | 0.75 | 0.99 |

Table 2 presents the overall performance metrics for skin cancer detection, that showcases the proposed LOCapsNet-XAI framework's notable improvements. The framework achieves increases of 6.35%, 9.98%, and 21.31% in accuracy; 7.25%,

12.19%, and 29.79% in precision; 8.23%, 10.93%, and 22.99% in specificity; 6.52%, 10.58%, and 21.35% in recall; and 6.89%, 11.39%, and 25.57% in F1-Score compared to existing models, including ResNet-18-XAI, EfficientNetV2S, and XceptionNet-

XAI, as well as CNN-Adam-RMSprop-XAI. Furthermore, the LOCapsNet-XAI framework demonstrates substantial reductions in computation time by 86.79%, 97.46%, and 96.907%, while also achieving improvements in AUC by 6.45%, 13.79%, and 32%. Its enhanced performance in key metrics positions it as a valuable tool for clinicians, especially given its efficiency for real-world applications. The integration of explainable AI also boosts its trustworthiness and applicability.

Looking ahead, future research will focus on further enhancing the diagnostic capabilities of LOCapsNet-XAI through integration with traditional diagnostic tools such as dermatoscopy and histopathology. This multimodal approach aims to provide a comprehensive assessment of skin lesions by leveraging visual insights from dermoscopy and cellular-level details from histopathological analysis. Combining the strengths of LOCapsNet-XAI in deep learning-based image classification with established methodologies of dermatoscopy and histopathology aims to improve diagnostic accuracy and facilitate earlier detection of skin cancer. This integrated framework broadens the scope of diagnostic evaluation and paves the way for personalized treatment plans. Ultimately this contributes to improved patient outcomes in dermatology.

CONCLUSION

The proposed LOCapsNet-XAI framework effectively integrated Convolutional Capsule Neural Networks optimized with the Ladybug Beetle Optimization algorithm (LOCapsNet) and Explainable AI (XAI) to enhance skin cancer classification using dermoscopic images. The systematic approach began with the collection of diverse multi-center clinical data to create a representative training dataset. Image preprocessing techniques such as Anisotropic Diffusion and Kuwahara Filtering enhanced image clarity by reducing noise while preserving important features. Feature extraction and skin cancer detection utilized the Convolutional Capsule Neural Network architecture to capture complex patterns and spatial relationships. The model's parameters were optimized using the Ladybug Beetle Optimization Algorithm to improve classification performance. Explainable AI methodologies including Grad-CAM++ provided visual insights into the model's decision-making processes, that fosters the clinician trust. The workflow culminated in the accurate classification of skin lesions as benign or malignant, that facilitates informed clinical decision-making. The framework achieved remarkable metrics, including increases of 6.35%, 9.98%, and 21.31% in accuracy; 7.25%, 12.19%, and 29.79% in precision; 8.23%, 10.93%, and 22.99% in specificity; 6.52%, 10.58%, and 21.35% in recall; and 6.89%, 11.39%, and 25.57% in F1-Score compared to existing models, including ResNet-18-XAI, EfficientNetV2S, and XceptionNet-XAI, as well as CNN-Adam-RMSprop-XAI. Furthermore, the LOCapsNet-XAI framework demonstrated substantial reductions in computation time by 86.79%, 97.46%, and 96.907%, while also achieving improvements in AUC by 6.45%, 13.79%, and 32%. The LOCapsNet-XAI framework not only enhanced diagnostic accuracy but also reduced the likelihood of false positives and negatives, thereby minimizing unnecessary procedures and anxiety for patients. The provision of real-time insights into the model's predictions further

empowered clinicians to make informed decisions regarding patient care. Looking ahead, the framework will be enriched through the integration of traditional diagnostic modalities, such as dermatoscopy and histopathology to provide a comprehensive assessment of skin lesions. Overall, the LOCapsNet-XAI framework represented a significant advancement in the realm of skin cancer classification, that paves the way for more effective, reliable, and patient-centered diagnostic solutions.

References

- Shah, A., Shah, M., Pandya, A., Sushra, R., Sushra, R., Mehta, M., Patel, K. and Patel, K., 2023. A comprehensive study on skin cancer detection using artificial neural network (ANN) and convolutional neural network (CNN). *Clinical eHealth*.
- Tembhurne, J.V., Hebbar, N., Patil, H.Y. and Diwan, T., 2023. Skin cancer detection using ensemble of machine learning and deep learning techniques. *Multimedia Tools and Applications*, 82(18), pp.27501-27524.
- Joel, R., Manikandan, G., Gokulaselvam, R., Bharath, R.K., Kumar, P. and Ebenezer, V., 2024. Convolutional neural networks and deep learning for the detection of pneumonia in X-RAY images. *ITEGAM-JETIA*, 10(49), pp.1-11.
- Bhuvanewari, G. and Manikandan, G., 2019. An intelligent intrusion detection system for secure wireless communication using IPSO and negative selection classifier. *Cluster Computing*, 22(Suppl 5), pp.12429-12441.
- Zhang, L., Zhang, J., Gao, W., Bai, F., Li, N. and Ghadimi, N., 2024. A deep learning outline aimed at prompt skin cancer detection utilizing gated recurrent unit networks and improved orca predation algorithm. *Biomedical Signal Processing and Control*, 90, p.105858.
- Venugopal, V., Raj, N.I., Nath, M.K. and Stephen, N., 2023. A deep neural network using modified EfficientNet for skin cancer detection in dermoscopic images. *Decision Analytics Journal*, 8, p.100278.
- Suresh, G., Bhuvanewari, G., Manikandan, G. and Shanthakumar, P., 2024. Chronological bald eagle optimization based deep learning for image watermarking. *Expert Systems with Applications*, 238, p.121545.
- Lembhe, A., Motarwar, P., Patil, R. and Elias, S., 2023. Enhancement in Skin Cancer Detection using Image Super Resolution and Convolutional Neural Network. *Procedia Computer Science*, 218, pp.164-173.
- Tabrizchi, H., Parvizpour, S. and Razmara, J., 2023. An improved VGG model for skin cancer detection. *Neural Processing Letters*, 55(4), pp.3715-3732.
- Bhuvanewari, G. and Manikandan, G., 2018. A novel machine learning framework for diagnosing the type 2 diabetics using temporal fuzzy ant miner decision tree classifier with temporal weighted genetic algorithm. *Computing*, 100, pp.759-772.
- Priyadarshini, N., Selvanathan, N., Hemalatha, B. and Sureshkumar, C., 2023. A novel hybrid Extreme Learning Machine and Teaching-Learning-Based Optimization algorithm for skin cancer detection. *Healthcare Analytics*, 3, p.100161.
- Manikandan, G. and Bhuvanewari, G., 2022. Knowledge discovery in data of prostate cancer by applying ensemble

- learning. Indian Journal of Computer Science and Engineering (IJCSE), e-ISSN, pp.0976-5166.
- Gomathi, E., Jayasheela, M., Thamarai, M. and Geetha, M., 2023. Skin cancer detection using dual optimization based deep learning network. Biomedical Signal Processing and Control, 84, p.104968.
- Ultanuddin, S.J., Kumar, A.G.D., Maithili, K., Vanguri, G.N., Padhi, M.K., Gangopadhyay, A., Bhuvaneshwari, G. and Manikandan, G., 2024. A Novel Support Vector Machine based Improved Aquila Optimizer-based Text Mining Mechanism for the Healthcare Applications. Journal of Electrical Systems, 20(3), pp.1430-1443.
- Gururaj, H.L., Manju, N., Nagarjun, A., Aradhya, V.M. and Flammini, F., 2023. DeepSkin: a deep learning approach for skin cancer classification. IEEE Access, 11, pp.50205-50214.
- Nigar, N., Umar, M., Shahzad, M.K., Islam, S. and Abalo, D., 2022. A deep learning approach based on explainable artificial intelligence for skin lesion classification. IEEE Access, 10, pp.113715-113725.
- Gautam, Y., Gupta, P., Kumar, D., Kalra, B., Kumar, A. and Hemanth, J.D., 2024. FusionEXNet: an interpretable fused deep learning model for skin cancer detection. International Journal of Computers and Applications, pp.1-11.
- Mridha, K., Uddin, M.M., Shin, J., Khadka, S. and Mridha, M.F., 2023. An interpretable skin cancer classification using optimized convolutional neural network for a smart healthcare system. IEEE Access, 11, pp.41003-41018.
- Khater, T., Ansari, S., Mahmoud, S., Hussain, A. and Tawfik, H., 2023. Skin cancer classification using explainable artificial intelligence on pre-extracted image features. Intelligent Systems with Applications, 20, p.200275.
- Attallah, O., 2024. Skin-CAD: Explainable deep learning classification of skin cancer from dermoscopic images by feature selection of dual high-level CNNs features and transfer learning. Computers in Biology and Medicine, 178, p.108798.
- Hosny, K.M., Said, W., Elmezain, M. and Kassem, M.A., 2024. Explainable deep inherent learning for multi-classes skin lesion classification. Applied Soft Computing, 159, p.111624.
- Priyanka Pramila, R. and Subhashini, R., 2023. Automated skin lesion detection and classification using fused deep convolutional neural network on dermoscopic images. Computational Intelligence, 39(6), pp.1073-1087.
- International Skin Imaging Collaboration (ISIC)-archive "<https://challenge.isic-archive.com/data/>", accessed in October 2024.
- HAM10000 dataset
"<https://www.kaggle.com/datasets/kmader/skin-cancer-mnist-ham10000>", accessed in October 2024.
- DermNet Dataset
"<https://www.kaggle.com/datasets/shubhamgoel27/dermnet>", accessed in October 2024.
- PH2-Dataset:
"<https://www.kaggle.com/datasets/athina123/ph2dataset>", accessed in October 2024.
- Kumar, M.P., Poornima, B., Nagendraswamy, H.S. and Manjunath, C., 2021. Structure-preserving NPR framework for image abstraction and stylization. The Journal of Supercomputing, 77(8), pp.8445-8513.
- Kabir, M.H., Hasan, M.A. and Shin, W., 2022. CSI-DeepNet: A lightweight deep convolutional neural network-based hand gesture recognition system using Wi-Fi CSI signal. IEEE Access, 10, pp.114787-114801.
- Safiri, S. and Nikoofard, A., 2023. Ladybug Beetle Optimization algorithm: application for real-world problems. The Journal of Supercomputing, 79(3), pp.3511-3560.